Article

Multi Resolution Analysis (MRA) of satellite images of oil spill disasters

Rashid Hussain

Faculty of Engineering Science and Technology, Hamdard University, Karachi 74600, Pakistan

E-mail: rashid.hussain@hamdard.edu.pk

Received 17 February 2014; *Accepted 25 March 2014*; *Published online 1 September 2014*

(cc) BY

Abstract

Oil spill disasters monitoring and mitigation requires availability of state of the art applications and tools. Conventional technology gets benefit from latest trends and research in satellite imaginary. This research highlights multi-resolution wavelet analysis of satellite images of oil spill disasters. Multi-resolution analysis is one of the powerful techniques to analyze information content of images. This analysis enables us to have a scale-invariant interpretation of the image. At each resolution level, both smooth and detailed signals carry all the necessary information to reconstruct the smooth signal at the next level. The wavelet decomposition results in detail and approximate threshold coefficients. Multi resolution wavelet decomposition is used to analyze the image in both time and frequency domain. It provides better frequency resolution and poor time resolution for lower frequency; better time resolution and poor frequency resolution for higher frequency. This condition is fortunately suited for real applications; as signals have high frequency components for very short period of the interval and low frequency components for longer durations.

Keywords remote sensing, multi-resolution wavelet analysis, satellite images of oil spill disasters.

Computational Ecology and Software
ISSN 2220-721X
URL: http://www.iaees.org/publications/journals/ces/online-version.asp
RSS: http://www.iaees.org/publications/journals/ces/rss.xml
E-mail: ces@iaees.org
Editor-in-Chief: WenJun Zhang
Publisher: International Academy of Ecology and Environmental Sciences

1 Introduction

Satellite images of oil spill disasters can be beneficial for various ecological and environmental predictions and monitoring. Some of the earlier research includes radar imagery of oil slicks, which can be valuable to extract information for monitoring and clean-ups the spills (Pilon and Purves, 1973). Recent researches in this domain includes: A statistical approach for automatic detection of ocean disturbance features from SAR images, in this statistical approach is applied to detects dark curvilinear features (Chaudhuri et al., 2012), Estimation of thickness of marine oil slicks from sun- glittered, near-infrared MERIS and MODIS Imagery (De Carolis et al., 2014), Oil spill mapping and measurement in the Gulf of Mexico with Textural Classifier Neural Network Algorithm (Garcia et al., 2013), A globally statistical active contour model for segmentation of oil slick in SAR Imagery (Song et al., 2013), Satellite oil spill detection using Artificial Neural Networks (Singha et al., 2013), remote sensing of ocean oil-spill pollution (Solberg et al., 2012) and SAR image quality assessment and

indicators for vessel and oil spill detection (Vespe and Greidanus, 2012).

In satellite images of oil spill disasters location and duration of different frequencies play an important role. To model certain activity, a signal can be obtained as a combination of small finite duration waves located at various spatial resolutions. The location of these short waves could be very vital for image processing. These types of problems cannot be fully analyzed by Fourier analysis alone. Several approaches have been devised to analyze the signal in time-frequency domain. In 1975, Jean Morlet coined the term "Wavelet" to describe his theory "Wavelet of Constant Slope" (Morlet et al., 1988). In 1981, Morlet together with Grossmann devised a method to synthesize and analyze an image without any loss of information. Morlet's research was a big breakthrough in underground oil exploration. In image compression, modern wavelet made use of Morlet's research to efficiently minimize and recompose wavelet coefficients (Morlet et al., 1988; Goupillaud et al., 1984).

In 1989, Stephane Mallat together with Meyer proposed a simple process which made wavelet more easier using multi resolution analysis (Mallat, 1989). One of the earlier attempts was known as the continuous wavelets transform (CWT) (Goupillaud et al., 1984). A CWT contains significant amount of redundancies which can be eliminated through discrete wavelet transforms (DWT). In 1988, Ingrid Daubechies made her well-known finding in the field of wavelet. Her research work led to the invention of a family of "compactly supported" wavelets. Daubechies' research work introduced a new system of image compression, which is capable of compressing the image without sacrificing the details of the image (Daubechies, 1988; Daubechies, 1992). The JPEG2000 file compression format is the result of her wavelets research framework. Recently Robinson proposed a research focused on combining power of Fourier and wavelet to restore and de-noise an image. In their method of Super-Resolution, multiple low quality images are combined to get high quality images (Robinson et al., 2010).

2 Multi-resolution Analysis (MRA)

The following section gives an understanding of wavelet multi-resolution theory (Mallat, 1989; Mallat, 1998; Goupillaud et al., 1984; Daubechies, 1988; Daubechies, 1992; Robinson et al., 2010).

Multi-resolution analysis is one of the powerful techniques to analyze information content of images. It provides analysis of the signal or image at different resolutions. By applying MRA to a signal, the feature that might go unnoticed at one resolution can be detected using a different resolution. In MRA scaling or approximation function $\varphi(2^{j/2}x-k)$ is used to create a series of the approximation of the signal or image, while the difference between two adjacent approximations is named as wavelet or detail function $\Psi\ (2^{j/2}x-k)$. Each new signal at next finer level *j+1*, is obtained as a sum of scaling or approximation function (local average) and wavelet or detail function (local difference) at level *j* (Gilbert and Nguyen, 1996), where *j* defines the width and *k* defines the position of the scaling $\psi_{j,k}(x)$ along x axis; *x* is discrete set of numbers starting from *x=0, 1,2….M-1*. Each neighbor is different from its adjacent neighbor by a factor of $2^{j/2}$. Scale and translated functions examine signal in Multi-resolution analysis by controlling the height and position of the mother wavelet, mathematically it is defined as (1) and (2):

$$\varphi_{j,k}(x) = 2^{j/2}\varphi(2^{j/2}x-k) \tag{1}$$

$$\Psi^{i}{}_{j,k}(x) = 2^{j/2}\,\Psi\ (2^{j/2}x - k) \tag{2}$$

2.1 Wavelet series expansions

The wavelet series expansions of function $f(x)$ relative to wavelet $\psi_{j,k}(x)$ and scaling function $\varphi_{j,k}(x)$ can be given as (3) and (4) (Mallat, 1989; Mallat, 1998; Goupillaud et al., 1984; Daubechies, 1988; Daubechies, 1992; Robinson et al., 2010).

$$f(x,y) = \sum_{k} c_{j_o}(k)\varphi_{j_o,k}(x) + \sum_{j=j_o}^{\infty}\ \sum_{k}\ d_j(k)\Psi_{j,k}(x) \tag{3}$$

scaling or approximation coefficients can be given as,

$$c_{j_o}(k) = \left\langle f(x), \varphi_{j_o,k}(x)\right\rangle = \int f(x)\varphi_{j_o,k}(x)dx \tag{4}$$

Wavelet or detail coefficients can be given as (5) [6-7],

$$d_j(k) = \left\langle f(x), \psi_{j_o,k}(x)\right\rangle = \int f(x)\psi_{j_o,k}(x)dx \tag{5}$$

2.2 Continuous wavelets transformation

The continuous wavelets transform (CWT) of a continuous function $f(x)$ is decomposed using wavelet $\psi_{s,\tau}(x)$, where *s* and τ are scaling and translation variables respectively. The resulting transform provides a new dimension to the function $f(x)$ for time-frequency or in other words time-scale analysis given as (6) (Gonzalez and Wood, 2002):

$$W_{\Psi}(s,\tau) = \int_{-\infty}^{\infty} f(x)\psi_{s,\tau}(x)dx \tag{6}$$

where

$$\psi_{s,\tau} = \frac{1}{\sqrt{s}}\psi\left(\frac{x-\tau}{s}\right) \tag{7}$$

The inverse continuous wavelets transform can be given as (8):

$$f(x) = \frac{1}{C_{\psi}}\int_{0}^{\infty}\int_{-\infty}^{\infty} W_{\Psi}(s,\tau)\frac{\psi_{s,\tau}(x)}{s^2}d\tau ds \tag{8}$$

$$C_{\Psi} = \int_{-\infty}^{\infty} \frac{|\psi(u)|^2}{|u|} du \tag{9}$$

where $C_{\Psi} < \infty$ define the admissibility criterion for reversible transform (Morlet et al., 1988) and $\psi(u)$ is the Fourier transformation of $\psi(x)$.

2.3 Discrete wavelets transformation

The continuous wavelet transform (CWT) is obtained by calculating the correlation between continuous function $f(x)$ and two highly continuous scaling *s* and translation τ variables of the wavelet $\psi_{s,\tau}(x)$. The resultant transform is highly redundant and this redundancy should be removed for most of the practical applications. The issue of redundancy can be limited by employing discrete wavelet. Instead of continuously computing continuous function $f(x)$ and two highly continuous scaling and translation τ variables, a transform is obtained using discrete steps. The Discrete wavelet transforms (DWT) is mathematically given as (10) (Gonzalez and Wood, 2002).

$$W_{\varphi}(j_o,k) = \frac{1}{\sqrt{M}} \sum_{x} f(x) \varphi_{j_o,k}(x) \tag{10}$$

(Approximation Coefficients)

where *j* defines the width and *k* defines the position of the scaling $\varphi_{j,k}(x)$ along *x* axis; *x* is a discrete set of numbers starting from *x = 0, 1, 2….M-1.*

$$W_{\psi}(j,k) = \frac{1}{\sqrt{M}} \sum_{x} f(x) \psi_{j,k}(x) \tag{11}$$

(Detail Coefficients)

The Inverse Discrete wavelet transforms (DWT) is mathematically given as (12):

$$f(x,y) = \frac{1}{\sqrt{M}} \sum_{k} W_{\varphi}(j_o,k) \varphi_{j_o,k}(x) + \frac{1}{\sqrt{M}} \sum_{j=j_o}^{\infty} \sum_{k} W_{\Psi}(j,k) \Psi_{j_o,k}(x) \tag{12}$$

2.4 2D-discrete wavelets transformation

Two dimensional (2D) discrete wavelets transformation can be represented using scaling function $\varphi(x,y)$ and three wavelet functions $\Psi(x,y)$. Wavelet variations across horizontal edges, vertical edges and diagonals are represented by Ψ^H, Ψ^V and Ψ^D respectively, which is given as (13) - (16) (Gonzalez and Wood, 2002).

$$\varphi(x,y)=\varphi(x)\varphi(y) \tag{13}$$

$$\Psi^{H}(x,y)=\Psi(x)\varphi(y) \tag{14}$$

$$\Psi^{V}(x,y)=\varphi(x)\Psi(y) \tag{15}$$

$$\Psi^{D}(x,y)=\Psi(x)\Psi(y) \tag{16}$$

2D scale and translated functions are further representing as (17)- (18):

$$\varphi_{j,m,n}(x,y)=2^{j/2}\varphi(2^{j/2}x-m,2^{j/2}y-n,) \tag{17}$$

$$\Psi^{i}{}_{j,m,n}(x,y)=2^{j/2}\Psi^{i}(2^{j/2}x-m,2^{j/2}y-n,) \tag{18}$$

where directional wavelets are represented by i = {H, V, D}. The DWT of the image function f(x, y) of size M x N is represented as (19)- (20),

$$W_{\varphi}(j_o,m,n)=\frac{1}{\sqrt{MN}}\sum_{x=0}^{M-1}\sum_{y=0}^{N-1}f(x,y)\varphi_{j_o,m,n}(x,y) \tag{19}$$

$$W_{\Psi}^{i}(j,m,n)=\frac{1}{\sqrt{MN}}\sum_{x=0}^{M-1}\sum_{y=0}^{N-1}f(x,y)\Psi^{i}{}_{j_o,m,n}(x,y) \tag{20}$$

Inverse Discrete wavelet Transform (IDWT) is performed to obtain the de-noised image using modified co-efficient without the loss of information. It reassembles a signal from the approximate and detail coefficients obtained from decomposition step.

Unlike DWT this process involves up-sampling (interpolating) and filtering. Mathematically the IDWT is given as (21) (Gonzalez and Wood, 2002),

$$f(x,y)=\frac{1}{\sqrt{MN}}\sum_{m}\sum_{n}W_{\varphi}(j_o,m,n)\varphi_{j_o,m,n}(x,y)+ \tag{21}$$
$$\frac{1}{\sqrt{MN}}\sum_{i=H,V,D}\sum_{j=j_o}^{\infty}\sum_{m}\sum_{m}W_{\Psi}^{i}(j,m,n)\Psi^{i}{}_{j_o,m,n}(x,y)$$

3 Procedures

The purpose of MRA is to give good time resolution and poor frequency resolution at high frequencies and good frequency resolution and poor time resolution at low frequencies. This approach makes sense especially

when the signal at hand has high frequency components for short durations and low frequency components for long durations. The signals that are encountered in practical applications are often of this type. The MRA analyzes the signal at different frequency bands with different resolutions by decomposing the signal into a coarse approximation and detail information MRA employs two sets of functions, called scaling functions and wavelet functions, which are associated with low pass and high pass filters, respectively.

The *LL1* subband comes from low pass filtering in both vertical and horizontal direction and it is called approximation (most like original picture).The remaining are called details subband or detail components. The *LH* subband comes from low pass filtering in horizontal direction and high pass filtering vertical direction. Level of decomposition plays an important role for satisfactory noise removal which in better signal to noise ratio SNR in the original signals. The process of obtaining the approximation and detail coefficient is termed as decomposition. During multilevel decomposition this process repeats over and over again (Fig. 1 and 2).

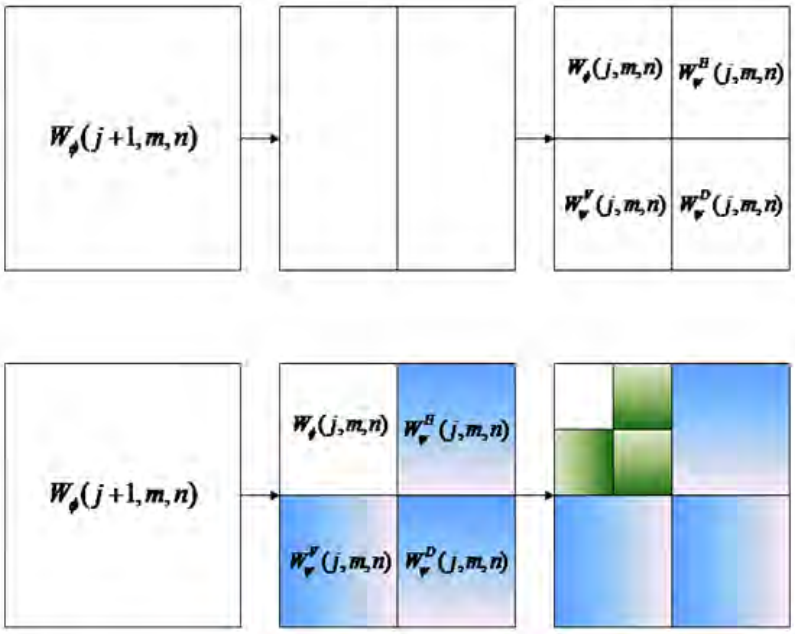

Fig. 1 Two-scale of two-dimensional decomposition (Gonzalez and Wood, 2002).

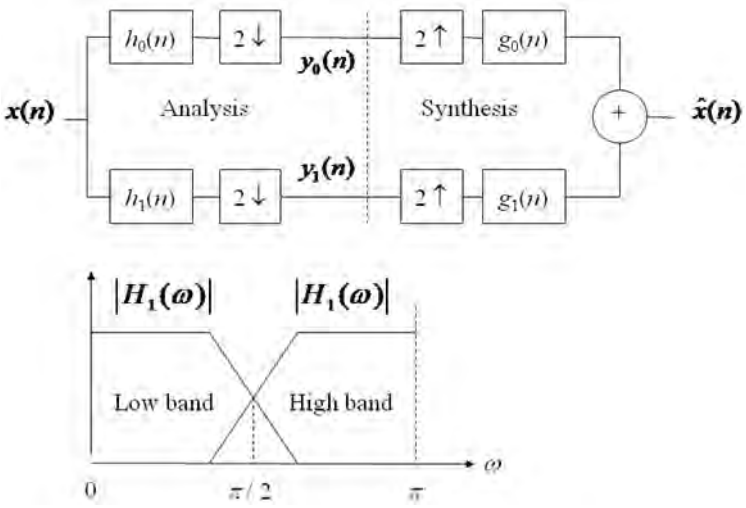

Fig. 2 Two-scale of two-dimensional decomposition (Gonzalez and Wood, 2002).

Successive lowpass/highpass filtering and downsampling on different level: capture transitions of different frequency bands on the same level: capture transitions at different locations. Wavelet transform breaks down a signal into a series of smooth signal and associated detailed signals at different resolution levels (Mallat, 1989). The purpose of this transformation is to represent the information of the signal, both in time and frequency domains in order to provide signal representation for further process. During multilevel decomposition, this process repeats over and over again, as shown in Fig. 3 and Fig. 4 (Mallat, 1989; Mallat, 1998; Goupillaud et al., 1984; Daubechies, 1988; Daubechies, 1992; Robinson et al., 2010).

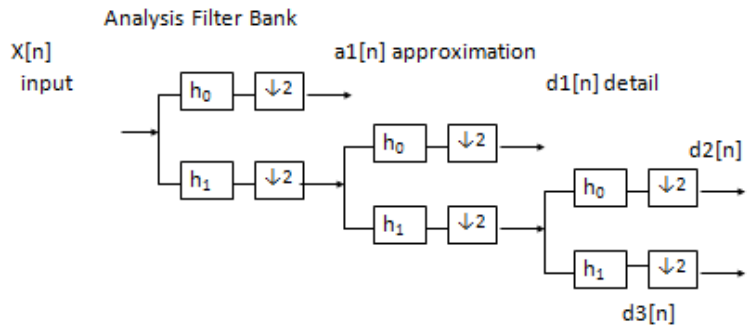

Fig. 3 Three-level wavelet decomposition tree (Gonzalez and Wood, 2002).

Fig. 3 is the analysis filter bank which decreases the rate of input signal and produces multiple output signals with varying rate; this decomposition is represented as the DWT of the signal. H0 and H1 are low and high pass filters respectively for analysis bank. Fig. 4 is the synthesis filter bank which increases the rate of multiple input signals and produces single output signals; this reconstruction is represented as the IDWT of the signal. G0 and G1 are low and high pass filters respectively for synthesis bank.

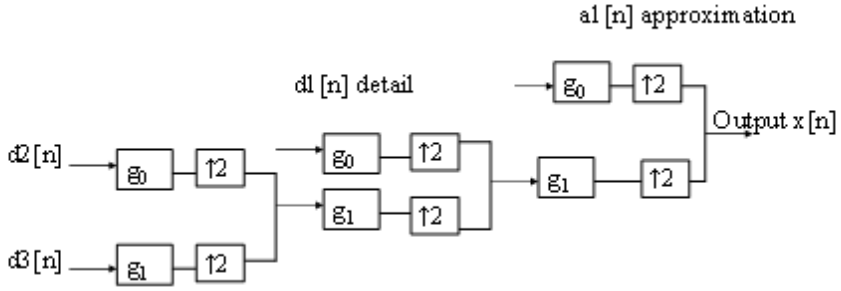

Fig. 4 Three-level wavelet reconstruction tree (Gonzalez and Wood, 2002).

4 Results and Discussion

To demonstrate multi-resolution analysis, this research includes single-level and multilevel decomposition and reconstruction. Fig. 5 represents how first level decomposition of images 1, images 2 and images 3 *is* translated into approximation *A1*, horizontal detail *H1*, vertical detail *V1* and diagonal detail *D1*. Fig. 6 shows how first and second level reconstructions of images are obtained using original image. Fig. 7 represents how multi level decomposition of *oil spill-2* is translated into approximation A1, horizontal detail H1, vertical detail V1 and diagonal detail D1, also how it is translated into approximation A2, horizontal detail H2, vertical detail V2 and diagonal detail D2.

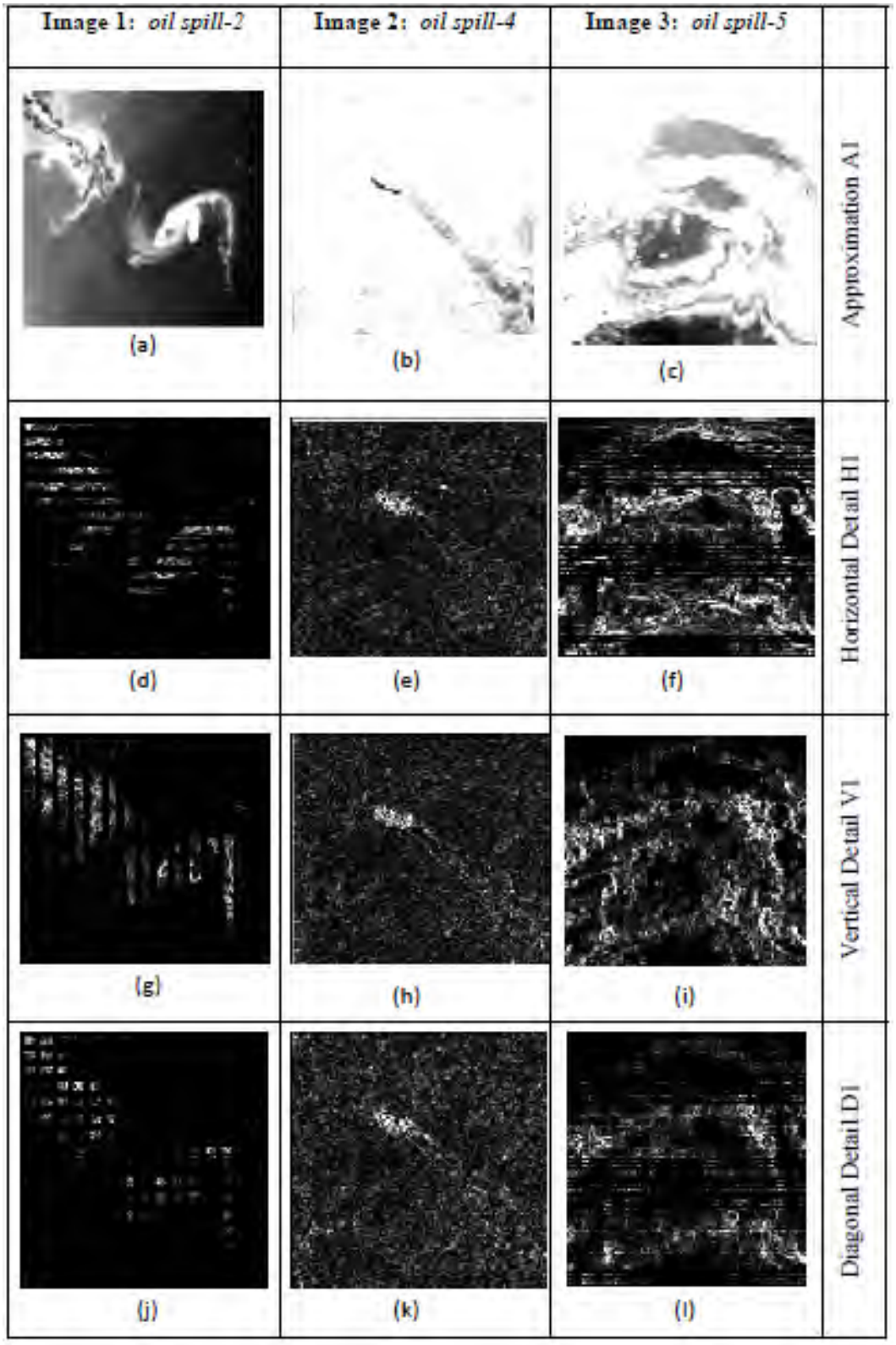

Fig. 5 First level decomposition of images 1, images 2 and images 3.

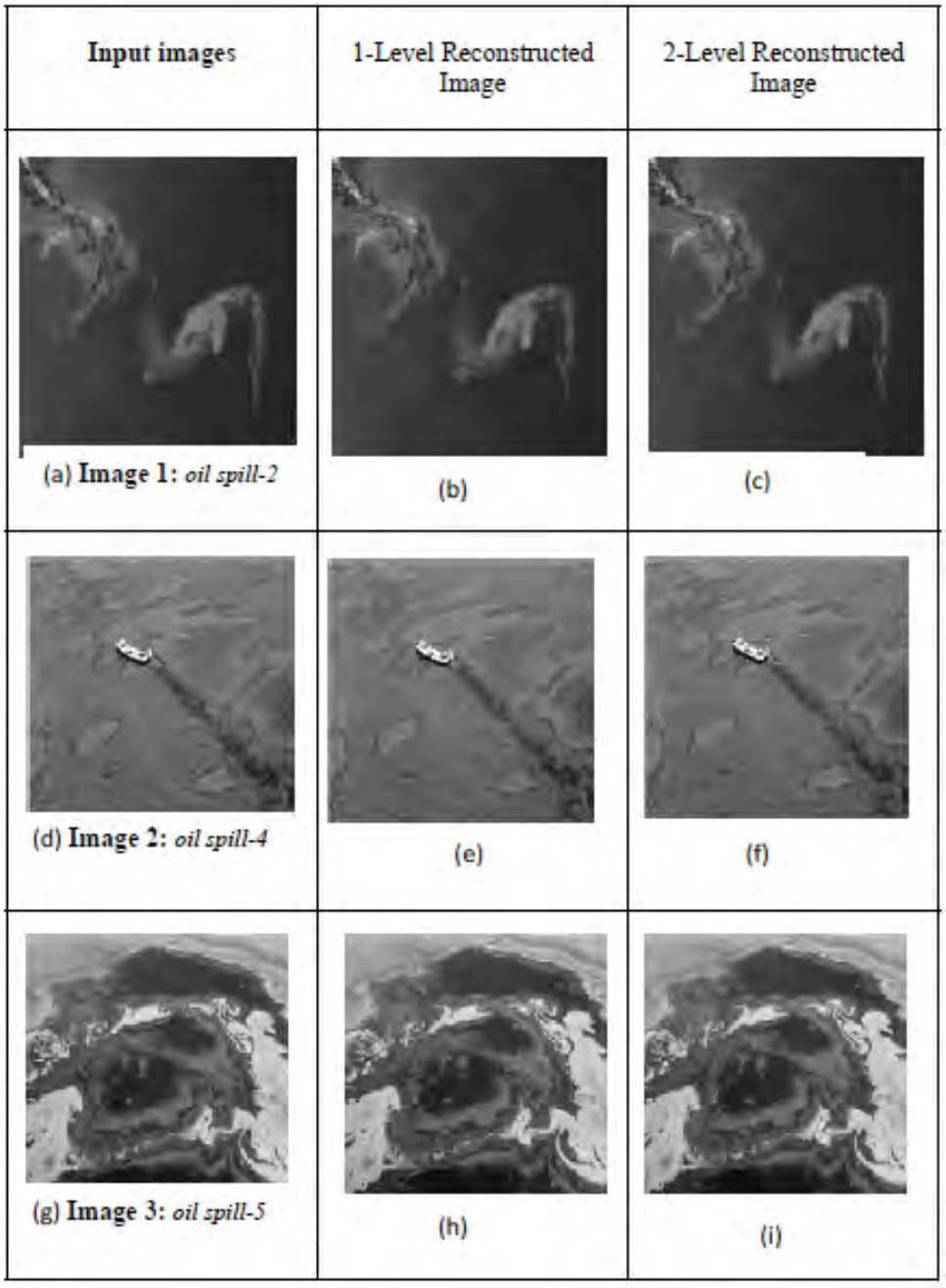

Fig. 6 First and Second level reconstruction of oil spill images.

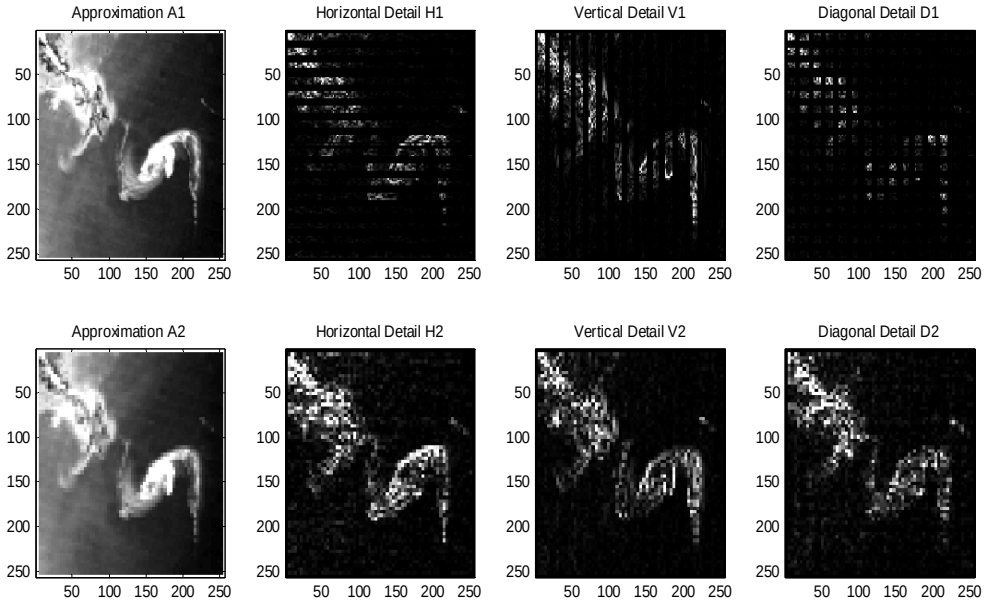

Fig. 7 Multi level Decomposition of image 1 *oil spill-2* a) Approximation A1 b) Horizontal Detail H1 c) Vertical Detail V1 d) Diagonal Detail D1 e) Approximation A2 f) Horizontal Detail H2 g) Vertical Detail V2 h) Diagonal Detail D2.

Mallat's theorem provides information on both spatial and frequency domain. Multi resolution analysis splits the signal in two sub-bands at the analysis side, and it offers perfect reconstruction at the reconstruction side, Mallat's powerful framework links the theory of wavelet to number techniques, including sub-band coding, quadrature mirror filtering and pyramidal coding (Mallat, 1989). However, such structured approach requires equally structured input (Stollnitz and Tony, 1996). The proposed research by Coupe Introduced 3D wavelet sub-band's mixing based on nonlocal mean filter for noise removal (Pierrick et al., 2008).

Table 1 Statistical Parameters for oil spill images.

Statistical Parameters	**Image 1**	**Image 2**	**Image 3**
Mean	72.76	115.3	94.9
Median	57	113	90
Mode	43.48	130.5	79.74
Standard Deviation	50.33	43.14	38.6
Median Abs. Deviation	12	26	21
Mean Abs. Deviation	29.67	33.3	28.77
L1 norm	1.431e+007	8.904e+007	1.888e+007
L2 norm	3.923e+004	1.082e+005	4.569e+004
Max norm	255	255	255

Table 1 shows the statistical parameters for oil spill images. In statistics, the median absolute deviation (MAD) is a robust measure of the variability of a univariate sample of quantitative data. The norm of a matrix is a scalar that gives some measure of the magnitude of the elements of the matrix. L1-norm is also known as least absolute deviations (LAD), least absolute errors (LAE). It is basically minimizing the sum of the absolute differences between the target value and the estimated values. The Euclidean distance is computed as a L2-norm, is the square root of the sum of the absolute values squared.

5 Conclusion

Oil spill is of the calamitous issues affecting the environment in general and marine life in particular. This research presents an import aspect of image processing of oil spill disasters that can be helpful for combating environmental calamities. Wavelets are the foundation for representing images in various degrees of resolution. Multi-resolution Analysis has been implemented to calculate approximate and detail components of the image. This research provides multi-resolution wavelet analysis for image reconstruction of oil spill disaster at various levels. This analysis enables us to observe various transients in spatial domain as well as in frequency domain. This approach could be used to identify patterns, which otherwise, goes undetected by visual assessments.

Acknowledgments

We would like to thank Gilbert Strang, Mallat S.G., Rafael Gonzalez, and David Donoho for providing theoretical framework for wavelet in image processing. We also wish to thank Jason Townsend from NASA for vast resources on satellite images of oil spill disasters. We also wish to thank M. Misiti, Y. Misiti from The MathWorks, Inc for facilitating Matlab based implementation of wavelet and to the Graduate School of Engineering Sciences and Information Technology, Hamdard University for their logistic support and services.

References

Chaudhuri D, Samal A, Agrawal A, et al. 2012. A statistical approach for automatic detection of ocean disturbance features from SAR Images. Selected Topics in Applied Earth Observations. IEEE Journal of Remote Sensing, 5(4): 1231-1242

Daubechies I. 1988. Orthonormal bases of compactly supported Wavelets. Communications on Pure and Applied Mathematics, 41(7): 909-996

Daubechies I. 1992. Ten Lectures on Wavelets (1st ed). Society for Industrial and Applied Mathematics, 198: 254-257

De Carolis G, Adamo M, Pasquariello G. 2014. On the estimation of thickness of marine oil slicks from sun-glittered.near-infrared MERIS and MODIS imagery: The Lebanon oil spill case study. IEEE Transactions on Geoscience and Remote Sensing, 52(1): 559-573

Garcia-Pineda O, MacDonald IR, Li XF, et al. 2013. Oil spill mapping and measurement in the gulf of mexico with textual classifier neural network algorithm (TCNNA). Selected Topics in Applied Earth Observations. IEEE Journal of Remote Sensing, 6(6): 2517-2525

Gilbert S, Truong N. 1996. Wavelets and Filter Banks. Wellesley-Cambridge Press, USA

Gonzalez R, Wood R. 2002. Digital Image Processing (2nd edition). Pearson Education Inc., USA

Goupillaud P, Grossmann A, Morlet J. 1984. Cycle-octave and related transforms in seismic signal analysis. Geo-exploration, 23: 85-102

Mallat SG. 1989. A theory for multi-resolution signal decomposition: the wavelet representation. IEEE

Transaction on Pattern Analysis and Machine Intelligence, 11(7): 674-693

Mallat SG. 1998. A Wavelet Tour of Signal Processing (2nd Edition). Academic Press, USA

Morlet J, Kronland-Martinet A, Grossman R. 1988. Reading and understanding continuous wavelet Transforms. In: Wavelets, Time-Frequency Methods and Phase Space. 2-22, Springer, Marseille, France

Pierrick C, Hellier P, Prima S, et al. 2008. 3D Wavelet sub-bands mixing for image de-noising. International Journal of Biomedical Imaging, 590183

Pilon RO, Purves CG. 1973. Radar imagenary of oil slicks. IEEE Transactions on Aerospace and Electronic Systems, 5: 630 -636

Robinson MD. 2010. Efficient Fourier-wavelet super-resolution. IEEE Transaction on Image Processing, 19(10): 2669-268

Singha S, Bellerby TJ, Trieschmann O. 2013. Satellite oil spill detection using artificial neural networks. Selected Topics in Applied Earth Observations. IEEE Journal of Remote Sensing, 6(6): 2355-2363

Solberg AHS. 2012. Remote sensing of ocean oil-spill pollution. Proceedings of the IEEE, 100(10): 2931-2945

Song HH, Huang B, Zhang KH. 2013. A Globally Statistical Active Contour Model for Segmentation of Oil Slick in SAR Imagery. IEEE Journal of Selected Topics in Applied Earth Observations and Remote Sensing, 6(6): 2402-2409

Stollnitz EJ, Tony D. 1996. Wavelets for Computer Graphics. Morgan Kauffman, San Francisco, USA

Vespe M, Greidanus H. 2012. SAR image quality assessment and indicators for vessel and oil spill detection. IEEE Transactions on Geoscience and Remote Sensing, 50(11): 4726-4734